

X-ray specular scattering from statistically rough surfaces: a novel theoretical approach based on the Green function formalism

F. N. Chukhovskii^a and A. M. Polyakov^{b*}

^aInstitute of Crystallography, The Russian Academy of Sciences, 117333 Moscow, Leninsky Prospect 59, Russian Federation, and ^bDepartment of Materials Science, National University of Science and Technology 'MISIS', 117279 Moscow, Leninsky Prospect 4, Russian Federation. Correspondence e-mail: apolyakov@misis.ru

The Green function formalism is applied to the problem of grazing-incidence small-angle X-ray scattering from statistically rough surfaces. Kirchhoff's integral equation is used to describe the X-ray wavefield propagation through a single rough surface separating vacuum and medium. Taking into account multiple diffuse X-ray scattering effects, the reflection $R^{\text{coh}}(\theta)$ and transmission $T^{\text{coh}}(\theta)$ coefficients of the specular wave are obtained using the Gaussian statistical model of rough surfaces in terms of the two-point height–height correlation function. In the limiting cases when the correlation length ξ is equal to zero or infinity, analytical formulae for the reflection $R^{\text{coh}}(\theta)$ and transmission $T^{\text{coh}}(\theta)$ coefficients of the specular wave are obtained. It is important that in the case $\xi \rightarrow \infty$ they coincide with the corresponding reflection $R^{\text{DW}}(\theta)$ and transmission $T^{\text{DW}}(\theta)$ coefficients related to the conventional Debye–Waller approximation for describing the grazing X-ray scattering from a rough surface. In the case of finite values of correlation length ξ the reflection $|R^{\text{coh}}(\theta)|^2$ and transmission $|T^{\text{coh}}(\theta)|^2$ scans are numerically calculated.

© 2010 International Union of Crystallography
Printed in Singapore – all rights reserved

1. Introduction

Over the last 20 years the scattering of short-wavelength radiation from rough surfaces and/or interfaces has been the object of a number of works [see, for example, Sinha *et al.* (1988), Holy *et al.* (1999), Bushuev *et al.* (2002), Nosik (2002), Lazzari (2002), Lomov *et al.* (2005), Sutyurin & Prokhorov (2006), Bridou *et al.* (2006), Hodroj *et al.* (2006), Schmidbauer *et al.* (2008), Zozulya *et al.* (2008) and Chukhovskii (2009); also the pioneering works of Yoneda (1963), Nevot & Croce (1980) and Petrashen' *et al.* (1983)].

Indeed, many experimental and theoretical studies of X-ray scattering from multilayer structures (MLSs) with rough surfaces and interfaces using the high-resolution X-ray reflectometry (HRXR) technique to date have been reported (Lomov *et al.*, 2005; Bridou *et al.*, 2006; Bushuev *et al.*, 2002; Sutyurin & Prokhorov, 2006; Chukhovskii, 2009). Most of them have been analyzed in terms of 'Debye–Waller factors', which modify the conventional Fresnel coefficients allowing the root-mean-square (r.m.s.) interface roughness σ to be deduced from the experimental HRXR angular scan data $|R^{\text{exp}}(\theta)|^2$, where θ is the grazing angle of the X-ray incidence.

At the same time, as was pointed out by Sinha and co-authors (Sinha *et al.*, 1988), the diffuse X-ray scattering is notably significant for describing the X-ray specular reflection and transmission and it is directly associated with the two-

point height–height correlation function $K_2(|\mathbf{x}|/\xi)$ for statistically rough surfaces. The two-point height–height correlation function $K_2(|\mathbf{x}|/\xi)$ is defined provided that $K_2(|\mathbf{x}|/\xi)|_{\mathbf{x}=0} = 1$ and $K_2(|\mathbf{x}|/\xi)|_{|\mathbf{x}|} = 0$, the vector $\mathbf{x} \equiv \mathbf{x}_1 - \mathbf{x}_2$ is directed along the averaged flat surface, and ξ is the correlation length.

Specifically, an estimate of the multiple diffuse X-ray scattering is essential if it concerns the quantitative analysis of the HRXR scan data $|R^{\text{exp}}(\theta)|^2$ to retrieve the macroscopic MLS parameters, including the surface and interface roughness.

In this paper we are dealing with the reflection and transmission phenomena of the specular wave in the case of grazing-incidence small-angle X-ray scattering from statistically rough surfaces. A new theoretical approach is proposed. It is based on the Green function formalism using Kirchhoff's integral equation for describing the X-ray wavefield propagation through a random rough surface separating vacuum and medium.

In §2, Kirchhoff's integral equations for the reflected and transmitted wavefield amplitudes are derived as a compound part of the Green function formalism to obtain their rigorous solutions in the form of expansion series.

In §3, the general solutions for the reflection and transmission coefficients of the specular wave are obtained by use of the Gaussian statistical model describing a rough surface in terms of the two-point surface height–height correlation

function and taking into account multiple diffuse X-ray scattering effects.

In §4 the reflection and transmission angular scans are numerically calculated for different correlation lengths ξ . A homogeneous medium is characterized by the complex electric susceptibility χ (up to a factor of 4π). In the case under consideration the X-ray wavelength λ is of the order of 0.1 nm, the complex value $\chi \equiv \text{Re}(\chi) + i \text{Im}(\chi)$, $\text{Re}(\chi) < 0$ and $\text{Im}(\chi) > 0$, $\text{Re}(\chi) \simeq -10^{-5}$ and $\text{Im}(\chi) \simeq 0.05|\text{Re}(\chi)|$ are assumed.

Special attention is paid for comparison of the calculated reflection $|R^{\text{coh}}(\theta)|^2$ and transmission $|T^{\text{coh}}(\theta)|^2$ scans versus the incidence angle θ with the corresponding ones related to the conventional Debye–Waller approximation (*cf.* de Boer, 1994, 1995; Kohn, 2003).

As is known, the retrieval of the surface and/or interface roughness from the experimental HRXR data is based on the Debye–Waller approximation for the reflection and transmission coefficients of the specular wave. The latter are the conventional Fresnel coefficients multiplied by the corresponding Debye–Waller factors (see, for example, Kohn, 2003; Chukhovskii, 2009).

The Fresnel coefficients modified by the Debye–Waller factors have some validity, even when rough surfaces do not approach a conventional model but instead approach the Gaussian statistical model based on the two-point height–height correlation function. While there are similarities with the conventional approach, there arises an essential difference: at large incidence angles, $\theta > \theta_{\text{Cr}} = |\text{Re}(\chi)|^{1/2}$, the smallness of the diffuse X-ray scattering is no longer a valid assumption (Sinha *et al.*, 1988). We shall show that multiple diffuse X-ray scattering effects are not negligible and notably influence the reflection and transmission coefficients of the specular wave especially outside the total reflection angle region, $\theta > \theta_{\text{Cr}}$.

2. Theoretical foundation for describing the grazing X-ray wavefield propagation through a rough surface

Let the incident plane wave $E_0(\mathbf{r}) = \exp(i\mathbf{k}_0\mathbf{r})$ impinge on a single rough surface that separates vacuum and medium (the incident plane-wavefield amplitude is assumed to be equal to unity, \mathbf{k}_0 is the incident wavevector, $|\mathbf{k}_0| = k$, where k is the wavenumber in a vacuum).

As a key point for proceeding further in the description of the grazing X-ray specular scattering we shall adopt the surface Kirchhoff's integral equation that describes the scalar electric wavefield $E(\mathbf{r})$ within a single surface-confined medium, namely,

$$E(\mathbf{r}) = \int d^2x \left[-E(\mathbf{r}_S) \nabla_{\mathbf{r}_S} G(\mathbf{r}, \mathbf{r}_S) + G(\mathbf{r}, \mathbf{r}_S) \nabla_{\mathbf{r}_S} E(\mathbf{r}_S) \right] \mathbf{n}_S. \quad (1a)$$

Herein, the Green (the spherical point-source wave) function in a medium is equal to

$$G(\mathbf{r}, \mathbf{r}_S) = \frac{-1 \exp(ik|\mathbf{r} - \mathbf{r}_S|)}{4\pi |\mathbf{r} - \mathbf{r}_S|}. \quad (1b)$$

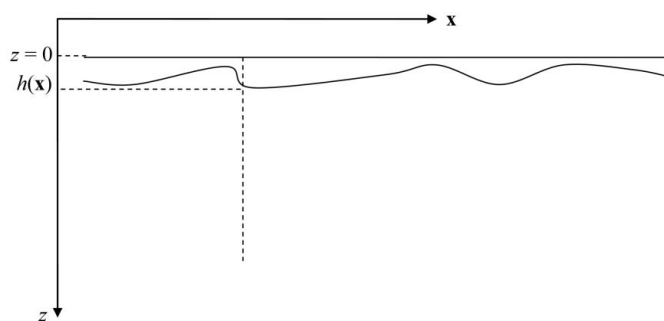


Figure 1

Rough surface schematic. The coordinate z is directed along the internal normal to the averaged flat surface $z = 0$. $h(\mathbf{x})$ is the height of a rough surface at point \mathbf{x} .

The radius vector \mathbf{r} determines the observation point in the medium. The radius vector \mathbf{r}_S determines a single rough surface, which has associated with it a random smooth one, $\mathbf{r}_S = \mathbf{x} + \mathbf{h}(\mathbf{x})$, the vector \mathbf{x} is along the average flat surface, $\mathbf{h}(\mathbf{x}) = h(\mathbf{x})\mathbf{n}_0$, \mathbf{n}_0 is the internal unit vector normal to the average flat surface, $\mathbf{x} \cdot \mathbf{h}(\mathbf{x}) = 0$ (Fig. 1). $h(\mathbf{x})$ is the height of the rough surface at point \mathbf{x} , the height function $h(\mathbf{x})$ is assumed to be single-valued. $\mathbf{n}_S = \mathbf{n}_0 + [h(\mathbf{x})/x_x]\mathbf{e}_x + [h(\mathbf{x})/x_y]\mathbf{e}_y$ is the internal vector normal to a rough surface at point \mathbf{r}_S and unit vectors \mathbf{e}_x and \mathbf{e}_y are directed along the x and z axes. $\kappa(\mathbf{r} - \mathbf{r}_S)/|\mathbf{r} - \mathbf{r}_S|$ is the wavevector of the spherical point-source wave in a medium, $\kappa^2 = k^2(1 + \chi)$. Noteworthy is the fact that the integration in (1) is carried out over the plane $\mathbf{r} \equiv (\mathbf{x}, 0)$ (the average flat surface).

The incident plane wave $E_0(\mathbf{r})$ initiates the transmitted wave $E_{\text{tran}}(\mathbf{r}) = T \exp(i\kappa\mathbf{r})$ [*cf.* equation (1a)] in a medium and the reflected wave $E_{\text{refl}}(\mathbf{r}) = R \exp(i\mathbf{k}_{\text{refl}}\mathbf{r})$ in a vacuum. The reflected wave $E_{\text{refl}}(\mathbf{r})$ and transmitted wave $E_{\text{tran}}(\mathbf{r})$ as functions of the radius vector \mathbf{r} are pseudo-plane waves and mainly depend on the exponential plane-wave factors $\exp(i\mathbf{k}_{\text{refl}}\mathbf{r})$ and $\exp(i\kappa\mathbf{r})$, where \mathbf{k}_{refl} and κ are the wavevector of the mirror-reflected and the transmitted plane waves for the case of the average flat surface, $z = 0$. In other words, $\mathbf{k}_{\text{refl}} \cdot \mathbf{n}_0 = -\mathbf{k}_0 \cdot \mathbf{n}_0 \equiv -k_{0z}$, $|\mathbf{k}_{\text{refl}}| = |\mathbf{k}_0|$ and $\kappa \times \mathbf{n}_0 = \mathbf{k}_0 \times \mathbf{n}_0$, $\kappa^2 = k^2$.

To be specific, the reflection $R(\mathbf{r})$ and transmission $T(\mathbf{r})$ amplitudes can be distinguished from the reflected $E_{\text{refl}}(\mathbf{r})$ and transmitted $E_{\text{tran}}(\mathbf{r})$ waves. Thus, as a result of the wavefield continuity along a surface, they are linked to each other as follows,

$$T[\mathbf{x} + \mathbf{h}(\mathbf{x})] \exp[i\kappa_z h(\mathbf{x})] = \exp[ik_{0z} h(\mathbf{x})] + R[\mathbf{x} + \mathbf{h}(\mathbf{x})] \exp[-ik_{0z} h(\mathbf{x})], \quad (2)$$

where the z component of the wavevector κ of the transmitted wave in a medium, $z > 0$, is equal to

$$\kappa_z = \kappa \mathbf{n}_0 = (k_{0z}^2 + \chi k^2)^{1/2}.$$

Using equations (1) and (2) for the wavefield at any point $\mathbf{r} = \mathbf{x} + \mathbf{h}(\mathbf{x})$, one obtains the integral equation for the reflected wave amplitude,

$$\begin{aligned}
 R[\mathbf{x} + \mathbf{h}(\mathbf{x})] = & -\exp[2ik_{0z}h(\mathbf{x})] + \int \exp[-i\mathbf{k}_0 \cdot (\mathbf{x} - \mathbf{x}_1)] \\
 & \times \left(\left\{ \nabla_{\mathbf{r}} G[\mathbf{x} - \mathbf{x}_1 + \mathbf{h}(\mathbf{x}) - \mathbf{h}(\mathbf{x}_1)] \right. \right. \\
 & + i\mathbf{k}_0 G[\mathbf{x} - \mathbf{x}_1 + \mathbf{h}(\mathbf{x}) - \mathbf{h}(\mathbf{x}_1)] \\
 & \times \mathbf{n}_{\mathbf{x}_1} \exp\{ik_{0z}[h(\mathbf{x}) + h(\mathbf{x}_1)]\} \\
 & + \left\{ \nabla_{\mathbf{r}} G[\mathbf{x} - \mathbf{x}_1 + \mathbf{h}(\mathbf{x}) - \mathbf{h}(\mathbf{x}_1)] \right. \\
 & + i\mathbf{k}_{\text{refl}} G[\mathbf{x} - \mathbf{x}_1 + \mathbf{h}(\mathbf{x}) - \mathbf{h}(\mathbf{x}_1)] \\
 & \times \mathbf{n}_{\mathbf{x}_1} \exp\{ik_{0z}[h(\mathbf{x}) - h(\mathbf{x}_1)]\} \\
 & \left. \left. \times R[\mathbf{x}_1 + \mathbf{h}(\mathbf{x}_1)] \right\} d^2\mathbf{x}_1. \quad (3)
 \end{aligned}$$

In deriving (3) we have utilized the fact that a gradient of the reflected wave amplitude $R[\mathbf{x} + \mathbf{h}(\mathbf{x})]$ can be neglected in comparison with a gradient of the exponential phase factor $\exp(i\mathbf{k}_{\text{refl}}\mathbf{r})$.

Further, the following substitution is utilized,

$$R[\mathbf{x} + \mathbf{h}(\mathbf{x})] = -\exp[2ik_{0z}h(\mathbf{x})] + \tilde{R}[\mathbf{x} + \mathbf{h}(\mathbf{x})], \quad (4)$$

where the ‘shifted’ reflection coefficient $\tilde{R}[\mathbf{x} + \mathbf{h}(\mathbf{x})]$ satisfies the following equation ($\mathbf{n}_{\mathbf{x}_1} \simeq \mathbf{n}_0$),

$$\begin{aligned}
 \tilde{R}[\mathbf{x} + \mathbf{h}(\mathbf{x})] = & 2ik_{0z} \int \exp[-i\mathbf{k}_0 \cdot (\mathbf{x} - \mathbf{x}_1)] \\
 & \times G[\mathbf{x} - \mathbf{x}_1 + \mathbf{h}(\mathbf{x}) - \mathbf{h}(\mathbf{x}_1)] \\
 & \times \exp\{ik_{0z}[h(\mathbf{x}) + h(\mathbf{x}_1)]\} d^2\mathbf{x}_1 \\
 & + \int \exp[-i\mathbf{k}_0 \cdot (\mathbf{x} - \mathbf{x}_1)] \\
 & \times \left\{ \nabla_{\mathbf{r}_S} G[\mathbf{x} - \mathbf{x}_1 + \mathbf{h}(\mathbf{x}) - \mathbf{h}(\mathbf{x}_1)] \right. \\
 & \left. - i\mathbf{k}_0 G[\mathbf{x} - \mathbf{x}_1 + \mathbf{h}(\mathbf{x}) - \mathbf{h}(\mathbf{x}_1)] \right\} \\
 & \times \mathbf{n}_0 \exp\{ik_{0z}[h(\mathbf{x}) - h(\mathbf{x}_1)]\} \\
 & \times \tilde{R}[\mathbf{x}_1 + \mathbf{h}(\mathbf{x}_1)] d^2\mathbf{x}_1. \quad (5a)
 \end{aligned}$$

Taking (2) into account, equation (5a) can be easily transformed to the integral equation for the transmitted wave amplitude, namely

$$\begin{aligned}
 T[\mathbf{x} + \mathbf{h}(\mathbf{x})] = & 2ik_{0z} \int \exp[-i\mathbf{k}_0 \cdot (\mathbf{x} - \mathbf{x}_1)] \\
 & \times G[\mathbf{x} - \mathbf{x}_1 + \mathbf{h}(\mathbf{x}) - \mathbf{h}(\mathbf{x}_1)] \\
 & \times \exp\{i[-\kappa_z h(\mathbf{x}) + k_{0z}h(\mathbf{x}_1)]\} d^2\mathbf{x}_1 \\
 & + \int \exp[-i\mathbf{k}_0 \cdot (\mathbf{x} - \mathbf{x}_1)] \\
 & \times \left\{ \nabla_{\mathbf{r}_S} G[\mathbf{x} - \mathbf{x}_1 + \mathbf{h}(\mathbf{x}) - \mathbf{h}(\mathbf{x}_1)] \right. \\
 & \left. - i\mathbf{k}_0 G[\mathbf{x} - \mathbf{x}_1 + \mathbf{h}(\mathbf{x}) - \mathbf{h}(\mathbf{x}_1)] \right\} \\
 & \times \mathbf{n}_0 \exp\{-i\kappa_z[h(\mathbf{x}) - h(\mathbf{x}_1)]\} \\
 & \times T[\mathbf{x}_1 + \mathbf{h}(\mathbf{x}_1)] d^2\mathbf{x}_1. \quad (5b)
 \end{aligned}$$

To solve equations (5a) and (5b) one applies the sequential iteration procedure. In its frame the formal rigorous solutions can be expanded in series as

$$\begin{aligned}
 \tilde{R}(\mathbf{r}_S) = & \int d^2\mathbf{x}_1 \exp[-i\mathbf{k}_0 \cdot (\mathbf{x} - \mathbf{x}_1)] \Omega_{\text{refl}}(\mathbf{r}_S, \mathbf{r}_{S,1}) \\
 & + \int d^2\mathbf{x}_1 \exp[-i\mathbf{k}_0 \cdot (\mathbf{x} - \mathbf{x}_1)] \Pi_{\text{refl}}(\mathbf{r}_S, \mathbf{r}_{S,1}) \\
 & \times \int d^2\mathbf{x}_2 \exp[-i\mathbf{k}_0 \cdot (\mathbf{x}_1 - \mathbf{x}_2)] \Omega_{\text{refl}}(\mathbf{r}_{S,1}, \mathbf{r}_{S,2}) \\
 & + \int d^2\mathbf{x}_1 \exp[-i\mathbf{k}_0 \cdot (\mathbf{x} - \mathbf{x}_1)] \Pi_{\text{refl}}(\mathbf{r}_S, \mathbf{r}_{S,1}) \\
 & \times \int d^2\mathbf{x}_2 \exp[-i\mathbf{k}_0 \cdot (\mathbf{x}_1 - \mathbf{x}_2)] \Pi_{\text{refl}}(\mathbf{r}_{S,1}, \mathbf{r}_{S,2}) \\
 & \times \int d^2\mathbf{x}_3 \exp[-i\mathbf{k}_0 \cdot (\mathbf{x}_2 - \mathbf{x}_3)] \Omega_{\text{refl}}(\mathbf{r}_{S,2}, \mathbf{r}_{S,3}) + \dots (6a)
 \end{aligned}$$

and

$$\begin{aligned}
 T(\mathbf{r}_S) = & \int d^2\mathbf{x}_1 \exp[-i\mathbf{k}_0 \cdot (\mathbf{x} - \mathbf{x}_1)] \Omega_{\text{tran}}(\mathbf{r}_S, \mathbf{r}_{S,1}) \\
 & + \int d^2\mathbf{x}_1 \exp[-i\mathbf{k}_0 \cdot (\mathbf{x} - \mathbf{x}_1)] \Pi_{\text{tran}}(\mathbf{r}_S, \mathbf{r}_{S,1}) \\
 & \times \int d^2\mathbf{x}_2 \exp[-i\mathbf{k}_0 \cdot (\mathbf{x}_1 - \mathbf{x}_2)] \Omega_{\text{tran}}(\mathbf{r}_{S,1}, \mathbf{r}_{S,2}) \\
 & + \int d^2\mathbf{x}_1 \exp[-i\mathbf{k}_0 \cdot (\mathbf{x} - \mathbf{x}_1)] \Pi_{\text{tran}}(\mathbf{r}_S, \mathbf{r}_{S,1}) \\
 & \times \int d^2\mathbf{x}_2 \exp[-i\mathbf{k}_0 \cdot (\mathbf{x}_1 - \mathbf{x}_2)] \Pi_{\text{tran}}(\mathbf{r}_{S,1}, \mathbf{r}_{S,2}) \\
 & \times \int d^2\mathbf{x}_3 \exp[-i\mathbf{k}_0 \cdot (\mathbf{x}_2 - \mathbf{x}_3)] \Omega_{\text{tran}}(\mathbf{r}_{S,2}, \mathbf{r}_{S,3}) + \dots, \quad (6b)
 \end{aligned}$$

where the functions $\Omega(\mathbf{r}_{S,n-1}, \mathbf{r}_{S,n})$ and $\Pi(\mathbf{r}_{S,n-1}, \mathbf{r}_{S,n})$ are defined by ($n = 1, 2, 3, \dots, \mathbf{r}_{S,0} \equiv \mathbf{r}_S$)

$$\begin{aligned}
 \Omega_{\text{refl}}(\mathbf{r}_{S,n-1}, \mathbf{r}_{S,n}) = & 2ik_{0z} \exp\{ik_{0z}[h(\mathbf{x}_{n-1}) + h(\mathbf{x}_n)]\} \\
 & \times G[\mathbf{x}_{n-1} - \mathbf{x}_n + \mathbf{h}(\mathbf{x}_{n-1}) - \mathbf{h}(\mathbf{x}_n)], \\
 \Pi_{\text{refl}}(\mathbf{r}_{S,n-1}, \mathbf{r}_{S,n}) = & \exp\{ik_{0z}[h(\mathbf{x}_{n-1}) - h(\mathbf{x}_n)]\} \\
 & \times \left\{ \nabla_{\mathbf{r}_{S,n-1}} G[\mathbf{x}_{n-1} - \mathbf{x}_n + \mathbf{h}(\mathbf{x}_{n-1}) - \mathbf{h}(\mathbf{x}_n)] \right. \\
 & \left. - i\mathbf{k}_0 G[\mathbf{x}_{n-1} - \mathbf{x}_n + \mathbf{h}(\mathbf{x}_{n-1}) - \mathbf{h}(\mathbf{x}_n)] \right\} \mathbf{n}_0 \quad (7a)
 \end{aligned}$$

and

$$\begin{aligned}
 \Omega_{\text{tran}}(\mathbf{r}_{S,n-1}, \mathbf{r}_{S,n}) = & 2i(\mathbf{k}_0 \cdot \mathbf{n}_0) \exp\{i[-\kappa h(\mathbf{x}_{n-1}) + k_{0z}h(\mathbf{x}_n)]\} \\
 & \times G[\mathbf{x}_{n-1} - \mathbf{x}_n + \mathbf{h}(\mathbf{x}_{n-1}) - \mathbf{h}(\mathbf{x}_n)], \\
 \Pi_{\text{tran}}(\mathbf{r}_{S,n-1}, \mathbf{r}_{S,n}) = & \exp\{-i\kappa[h(\mathbf{x}_{n-1}) - h(\mathbf{x}_n)]\} \\
 & \times \left\{ \nabla_{\mathbf{r}_{S,n-1}} G[\mathbf{x}_{n-1} - \mathbf{x}_n + \mathbf{h}(\mathbf{x}_{n-1}) - \mathbf{h}(\mathbf{x}_n)] \right. \\
 & \left. - i\mathbf{k}_0 G[\mathbf{x}_{n-1} - \mathbf{x}_n + \mathbf{h}(\mathbf{x}_{n-1}) - \mathbf{h}(\mathbf{x}_n)] \right\} \mathbf{n}_0. \quad (7b)
 \end{aligned}$$

It should be mentioned that each n -order term within the expansion series (6a), (6b) for obtaining the wave amplitudes $\tilde{R}(\mathbf{r}_S)$, $T(\mathbf{r}_S)$ is related to the multiple n -order re-emergence of the spherical point-source waves along a rough surface.

To describe the grazing-incidence small-angle X-ray specular scattering from statistically rough surfaces, one needs to move from the wave amplitude solutions (6a), (6b) to the reflection $\tilde{R}^{\text{coh}} = \langle \tilde{R}[\mathbf{x} + \mathbf{h}(\mathbf{x})] \rangle$ and transmission $T^{\text{coh}} = \langle T[\mathbf{x} + \mathbf{h}(\mathbf{x})] \rangle$ coefficients, where the notation $\langle \dots \rangle$ means a statistical average of the wave amplitudes.

It follows from some physical speculations that the two-point height–height correlation function

$$K_2(|\mathbf{x} - \mathbf{s}|/\xi) = \frac{\langle h(\mathbf{x})h(\mathbf{s}) \rangle}{[h^2(\mathbf{x})]^{1/2}[h^2(\mathbf{s})]^{1/2}}$$

is of great importance for deriving the coefficients R^{coh} and T^{coh} .

Then, we assume that the two-point surface height–height combinations of $[h(\mathbf{x}) \mp h(\mathbf{s})]$ are statistically independent Gaussian random variables. The statistical averages of the two-point height–height combinations $[h(\mathbf{x}) \mp h(\mathbf{s})]^2$ take the form (see, for example, Sinha *et al.*, 1988)

$$\langle [h(\mathbf{x}) \mp h(\mathbf{s})]^2 \rangle = 2\sigma^2 [1 \mp K_2(|\mathbf{x} - \mathbf{s}|/\xi)], \quad (8)$$

where the r.m.s. surface roughness σ and correlation length ξ are introduced.

Note that in the computer simulations below we shall assume that the coordinate dependence of the correlation function $K_2(x)$ has the exponential form $K_2(x) = \exp(-x)$. At the same time, the statistical model of independent height–height combinations allows us to find the basic solutions for reflection \tilde{R}^{coh} and transmission T^{coh} coefficients.

Correspondingly, after straightforward calculations one can obtain

$$\tilde{R}^{\text{coh}} \cong \frac{\int d^2\mathbf{s} \exp[-i\mathbf{k}_0 \cdot (\mathbf{x} - \mathbf{s})] \Omega_{\text{refl}}^{\text{coh}}(|\mathbf{x} - \mathbf{s}|)}{1 - \int d^2\mathbf{s} \exp[-i\mathbf{k}_0 \cdot (\mathbf{x} - \mathbf{s})] \Pi_{\text{refl}}^{\text{coh}}(|\mathbf{x} - \mathbf{s}|)} \quad (9)$$

and

$$T^{\text{coh}} \cong \frac{\int d^2\mathbf{s} \exp[-i\mathbf{k}_0(\mathbf{x} - \mathbf{s})] \Omega_{\text{tran}}^{\text{coh}}(|\mathbf{x} - \mathbf{s}|)}{1 - \int d^2\mathbf{s} \exp[-i\mathbf{k}_0(\mathbf{x} - \mathbf{s})] \Pi_{\text{tran}}^{\text{coh}}(|\mathbf{x} - \mathbf{s}|)}. \quad (10)$$

Herein, the average functions $\Omega^{\text{coh}}(|\mathbf{x} - \mathbf{s}|)$ and $\Pi^{\text{coh}}(|\mathbf{x} - \mathbf{s}|)$ involved in (9) and (10) are defined as follows,

$$\begin{aligned} \Omega_{\text{refl}}^{\text{coh}}(|\mathbf{x} - \mathbf{s}|) &= \langle \Omega_{\text{refl}}[|\mathbf{x} + \mathbf{h}(\mathbf{x}), \mathbf{s} + \mathbf{h}(\mathbf{s})|] \rangle, \\ \Pi_{\text{refl}}^{\text{coh}}(|\mathbf{x} - \mathbf{s}|) &= \langle \Pi_{\text{refl}}[|\mathbf{x} + \mathbf{h}(\mathbf{x}), \mathbf{s} + \mathbf{h}(\mathbf{s})|] \rangle \end{aligned} \quad (11)$$

and

$$\begin{aligned} \Omega_{\text{tran}}^{\text{coh}}(|\mathbf{x} - \mathbf{s}|) &= \langle \Omega_{\text{tran}}[|\mathbf{x} + \mathbf{h}(\mathbf{x}), \mathbf{s} + \mathbf{h}(\mathbf{s})|] \rangle, \\ \Pi_{\text{tran}}^{\text{coh}}(|\mathbf{x} - \mathbf{s}|) &= \langle \Pi_{\text{tran}}[|\mathbf{x} + \mathbf{h}(\mathbf{x}), \mathbf{s} + \mathbf{h}(\mathbf{s})|] \rangle. \end{aligned} \quad (12)$$

Evaluating the average functions (11) and (12) is a starting point for proceeding further in the description of the grazing X-ray specular scattering from statistically rough surfaces.

3. Reflection R^{coh} and transmission T^{coh} coefficients: the statistical model of a rough surface based on the two-point height–height correlation function

To calculate the reflection R^{coh} and transmission T^{coh} coefficients we will apply the two-dimensional Fourier transform of the spherical point-source wavefunction $G(\mathbf{r})$ in a medium [cf. equation (1b)],

$$G(\mathbf{r}) = -\frac{i}{8\pi^2} \int d^2\mathbf{p} \frac{\exp[i\mathbf{p} \cdot \mathbf{x} + i(\kappa^2 - \mathbf{p}^2)^{1/2}|z|]}{(\kappa^2 - \mathbf{p}^2)^{1/2}}. \quad (13)$$

Substituting the Fourier transform (13) into equations (9)–(12) and performing straightforward calculations, the reflection R^{coh} and transmission T^{coh} coefficients can be cast in the form

$$R^{\text{coh}} = -\langle \exp[2ik_{0z}h(\mathbf{x})] \rangle + \frac{\Omega_{\text{refl}}^{\text{coh}}}{1 - \Pi_{\text{refl}}^{\text{coh}}}, \quad (14)$$

$$T^{\text{coh}} = \frac{\Omega_{\text{tran}}^{\text{coh}}}{1 - \Pi_{\text{tran}}^{\text{coh}}}, \quad (15)$$

where the coefficients $\Omega_{\text{refl}}^{\text{coh}}$, $\Pi_{\text{refl}}^{\text{coh}}$, $\Omega_{\text{tran}}^{\text{coh}}$ and $\Pi_{\text{tran}}^{\text{coh}}$ involved in (14) and (15) are properly determined by

$$\begin{aligned} \Omega_{\text{refl}}^{\text{coh}} &= \frac{1}{4\pi^2} \int d^2\mathbf{s} \int d^2\mathbf{p} \frac{k_{0z} \exp[i(\mathbf{k}_0 - \mathbf{p}) \cdot (\mathbf{s} - \mathbf{u})]}{(\kappa^2 - \mathbf{p}^2)^{1/2}} \\ &\times \left\langle \exp \left\{ i(\kappa^2 - \mathbf{p}^2)^{1/2} |h(\mathbf{u}) - h(\mathbf{s})| \right. \right. \\ &\left. \left. + ik_{0z}[h(\mathbf{u}) + h(\mathbf{s})] \right\} \right\rangle, \end{aligned} \quad (16a)$$

$$\begin{aligned} \Pi_{\text{refl}}^{\text{coh}} \Big|_{\varepsilon \rightarrow +0} &= \frac{1}{8\pi^2} \int d^2\mathbf{s} \int d^2\mathbf{p} \\ &\times \left\{ \text{Sign}[\varepsilon + h(\mathbf{u}) - h(\mathbf{s})] - \frac{k_{0z}}{(\kappa^2 - \mathbf{p}^2)^{1/2}} \right\} \\ &\times \exp[i(\mathbf{k}_0 - \mathbf{p}) \cdot (\mathbf{s} - \mathbf{u})] \\ &\times \left\langle \exp \left\{ i(\kappa^2 - \mathbf{p}^2)^{1/2} |h(\mathbf{u}) - h(\mathbf{s})| \right. \right. \\ &\left. \left. + ik_{0z}[h(\mathbf{u}) - h(\mathbf{s})] \right\} \right\rangle, \end{aligned} \quad (16b)$$

and

$$\begin{aligned} \Omega_{\text{tran}}^{\text{coh}} &= \frac{1}{4\pi^2} \int d^2\mathbf{s} \int d^2\mathbf{p} \frac{k_{0z} \exp[i(\mathbf{k}_0 - \mathbf{p}) \cdot (\mathbf{s} - \mathbf{u})]}{(\kappa^2 - \mathbf{p}^2)^{1/2}} \\ &\times \left\langle \exp \left\{ i(\kappa^2 - \mathbf{p}^2)^{1/2} |h(\mathbf{u}) - h(\mathbf{s})| \right. \right. \\ &\left. \left. + i[-\kappa_z h(\mathbf{u}) + k_{0z} h(\mathbf{s})] \right\} \right\rangle, \end{aligned} \quad (17a)$$

$$\begin{aligned} \Pi_{\text{tran}}^{\text{coh}} \Big|_{\varepsilon \rightarrow +0} &= \frac{1}{8\pi^2} \int d^2\mathbf{s} \int d^2\mathbf{p} \\ &\times \left\{ \text{Sign}[\varepsilon + h(\mathbf{u}) - h(\mathbf{s})] - \frac{k_{0z}}{(\kappa^2 - \mathbf{p}^2)^{1/2}} \right\} \\ &\times \exp[i(\mathbf{k}_0 - \mathbf{p}) \cdot (\mathbf{s} - \mathbf{u})] \\ &\times \left\langle \exp \left\{ i(\kappa^2 - \mathbf{p}^2)^{1/2} |h(\mathbf{u}) - h(\mathbf{s})| \right. \right. \\ &\left. \left. - ik_z[h(\mathbf{u}) - h(\mathbf{s})] \right\} \right\rangle. \end{aligned} \quad (17b)$$

Before proceeding further, a few additional comments are appropriate concerning some of the theoretical aspects of implementing the theoretical approach presented here.

Firstly, to ensure the correct values of the reflection and transmission coefficients in the case of the ideally flat surface $z = 0$, in this case a random height function $h(\mathbf{x}) \equiv 0$, the parameter $\varepsilon \rightarrow +0$ is introduced [see formulae (16b) and (17b), ε can be put equal to the X-ray wavelength λ without losing its physical sense].

Then, in the case of $h(\mathbf{x}) = 0$, equations (16) and (17) directly yield

$$\Omega_{\text{refl}}^{\text{coh}} = \Omega_{\text{tran}}^{\text{coh}} = \frac{k_{0z}}{\kappa_z}$$

and

$$\Pi_{\text{refl}}^{\text{coh}} \equiv \Pi_{\text{tran}}^{\text{coh}} = \frac{1}{2} \frac{\kappa_z - k_{0z}}{\kappa_z}.$$

For this, according to (14) and (15) the reflection and transmission coefficients become the conventional Fresnel reflection and transmission ones, namely

$$R^{\text{coh}} = R^{\text{Fres}} \equiv \frac{k_{0z} - \kappa_z}{\kappa_z + k_{0z}}$$

and

$$T^{\text{coh}} = T^{\text{Fres}} \equiv \frac{2k_{0z}}{\kappa_z + k_{0z}}.$$

Secondly, in the limit case of correlation length $\xi \rightarrow \infty$, formulae (14)–(17) yield, provided that the r.m.s surface roughness $\sigma \neq 0$,

$$R^{\text{coh}} = f_R R^{\text{Fres}}$$

and

$$T^{\text{coh}} = f_T T^{\text{Fres}},$$

where the Debye–Waller factors $f_R = \exp(-2k_{0z}^2\sigma^2)$ and $f_T = \exp[-(k_{0z} - \kappa_z)^2/2\sigma^2]$. As mentioned above, the Debye–Waller approximations for the reflection R^{coh} and transmission T^{coh} coefficients are widely used for quantitative analysis of the HRXR scan data $|R^{\text{exp}}(\theta)|^2$ (see, for example, de Boer, 1994, 1995; Kohn, 2003; Chukhovskii, 2009).

Thirdly, it is notably important that the architecture of the general equations (14)–(17) is linked to the influence of multiple diffuse X-ray scattering effects upon the reflection and transmission coefficients of the specular wave.

It is clear from the physical viewpoint that the Debye–Waller approximation does work well at small angles $\theta \leq \theta_{\text{Cr}}$, at least, and in particular, in the case of correlation lengths $\xi \gg l$, where l is the X-ray absorption length in a medium, $l = \lambda/[2\pi\text{Im}(\chi)]$.

It is noteworthy that at large incidence angles $\theta > \theta_{\text{Cr}}$ the multiple diffuse X-ray scattering effects notably influence the reflection and transmission coefficients of the specular wave depending on the finite value of the correlation length ξ . It can be *a priori* stated that such an influence should increase (decrease) with increasing (decreasing) r.m.s. roughness σ .

4. Gaussian statistical model of a rough surface based on the two-point height–height correlation function: results and discussion

Applying the Gaussian statistical model *via* the two-point height–height correlation function (8) allows us to explicitly carry out an averaging procedure of terms involved on the right-hand sides of integrals (16) and (17).

Indeed, introducing the ‘combined’ r.m.s. roughness $\sigma_2(|\mathbf{u} - \mathbf{s}|) \equiv \sigma[1 - K_2(|\mathbf{u} - \mathbf{s}|/\xi)]^{1/2}$ to avoid bulky formulae, the straightforward calculations for such averages yield [*cf.* equations (16)–(17)]

$$\begin{aligned} \langle \exp[2ik_{0z}h(\mathbf{u})] \rangle &= \exp(-2k_{0z}^2\sigma^2), \\ \langle \exp \left\{ i(\kappa^2 - \mathbf{p}^2)^{1/2} |h(\mathbf{u}) - h(\mathbf{s})| + ik_{0z}[h(\mathbf{u}) + h(\mathbf{s})] \right\} \rangle \\ &= \exp(-2k_{0z}^2\sigma^2) \exp[-(\kappa^2 - \mathbf{p}^2 + k_{0z}^2)\sigma_2^2(|\mathbf{u} - \mathbf{s}|)] \\ &\quad \times \text{Erfc} \left[-i\sigma_2(|\mathbf{u} - \mathbf{s}|)(\kappa^2 - \mathbf{p}^2)^{1/2} \right], \end{aligned} \quad (18a)$$

$$\begin{aligned} \langle \text{Sign}[\varepsilon + h(\mathbf{u}) - h(\mathbf{s})] \exp \left\{ i(\kappa^2 - \mathbf{p}^2)^{1/2} |h(\mathbf{u}) - h(\mathbf{s})| \right. \\ \left. + ik_{0z}[h(\mathbf{u}) - h(\mathbf{s})] \right\} \rangle \\ = \frac{1}{2} \left(\exp \left\{ -\sigma_2^2(|\mathbf{u} - \mathbf{s}|) \left[(\kappa^2 - \mathbf{p}^2)^{1/2} + k_{0z} \right]^2 \right\} \right. \\ \times \text{Erfc} \left\{ -\frac{\varepsilon}{2\sigma_2(|\mathbf{u} - \mathbf{s}|)} - i\sigma_2(|\mathbf{u} - \mathbf{s}|) \left[(\kappa^2 - \mathbf{p}^2)^{1/2} + k_{0z} \right] \right\} \\ \left. - \exp \left\{ -\sigma_2^2(|\mathbf{u} - \mathbf{s}|) \left[(\kappa^2 - \mathbf{p}^2)^{1/2} - k_{0z} \right]^2 \right\} \right. \\ \left. \times \text{Erfc} \left\{ \frac{\varepsilon}{2\sigma_2(|\mathbf{u} - \mathbf{s}|)} - i\sigma_2(|\mathbf{u} - \mathbf{s}|) \left[(\kappa^2 - \mathbf{p}^2)^{1/2} - k_{0z} \right] \right\} \right) \end{aligned} \quad (18b)$$

and

$$\begin{aligned} \langle \exp \left\{ i(\kappa^2 - \mathbf{p}^2)^{1/2} |h(\mathbf{u}) - h(\mathbf{s})| + i[-\kappa_z h(\mathbf{u}) + k_{0z} h(\mathbf{s})] \right\} \rangle \\ = \exp \left[-\frac{\sigma^2(\kappa_z - k_{0z})^2}{2} \right] \exp \left[-\frac{\sigma_2^2(|\mathbf{u} - \mathbf{s}|)(\kappa_z - k_{0z})^2}{4} \right] \\ \times \frac{1}{2} \left(\exp \left\{ -\sigma_2^2(|\mathbf{u} - \mathbf{s}|) \left[(\kappa^2 - \mathbf{p}^2)^{1/2} - \frac{k_{0z} + \kappa_z}{2} \right]^2 \right\} \right. \\ \times \text{Erfc} \left\{ -i\sigma_2(|\mathbf{u} - \mathbf{s}|) \left[(\kappa^2 - \mathbf{p}^2)^{1/2} - \frac{k_{0z} + \kappa_z}{2} \right] \right\} \\ \left. + \exp \left\{ -\sigma_2^2(|\mathbf{u} - \mathbf{s}|) \left[(\kappa^2 - \mathbf{p}^2)^{1/2} + \frac{k_{0z} + \kappa_z}{2} \right]^2 \right\} \right. \\ \left. \times \text{Erfc} \left\{ -i\sigma_2(|\mathbf{u} - \mathbf{s}|) \left[(\kappa^2 - \mathbf{p}^2)^{1/2} + \frac{k_{0z} + \kappa_z}{2} \right] \right\} \right), \end{aligned} \quad (19a)$$

$$\begin{aligned} \langle \text{Sign}[\varepsilon + h(\mathbf{u}) - h(\mathbf{s})] \exp \left\{ i(\kappa^2 - \mathbf{p}^2)^{1/2} |h(\mathbf{u}) - h(\mathbf{s})| \right. \\ \left. - i\kappa_z[h(\mathbf{u}) - h(\mathbf{s})] \right\} \rangle \\ = \frac{1}{2} \left(\exp \left\{ -\sigma_2^2(|\mathbf{u} - \mathbf{s}|) \left[(\kappa^2 - \mathbf{p}^2)^{1/2} - \kappa_z \right]^2 \right\} \right. \\ \times \text{Erfc} \left\{ -\frac{\varepsilon}{2\sigma_2(|\mathbf{u} - \mathbf{s}|)} - i\sigma_2(|\mathbf{u} - \mathbf{s}|) \left[(\kappa^2 - \mathbf{p}^2)^{1/2} - \kappa_z \right] \right\} \\ \left. - \exp \left\{ -\sigma_2^2(|\mathbf{u} - \mathbf{s}|) \left[(\kappa^2 - \mathbf{p}^2)^{1/2} + \kappa_z \right]^2 \right\} \right. \\ \left. \times \text{Erfc} \left\{ \frac{\varepsilon}{2\sigma_2(|\mathbf{u} - \mathbf{s}|)} - i\sigma_2(|\mathbf{u} - \mathbf{s}|) \left[(\kappa^2 - \mathbf{p}^2)^{1/2} + \kappa_z \right] \right\} \right). \end{aligned} \quad (19b)$$

Herein there is the complementary error function $\text{Erfc}(z)$ for complex z on the right-hand sides of averages (18) and (19).

In the next step towards obtaining the reflection and transmission coefficients, these averages have to be substituted into (16) and (17).

Moving from the momentum component variable p_x to the variable $q = p_x - k_{0x}$ within the mirror-scattering plane and neglecting the quadratic terms of p_x^2 , p_y^2 and of the term $(\kappa^2 - \mathbf{p}^2)^{1/2}$ involved in (16)–(19), we obtain ultimately

$$\begin{aligned} \Omega_{\text{refl}}^{\text{coh}} &= \frac{\exp(-2k_{0z}^2\sigma^2)}{\pi} \int_{-\infty}^{\infty} dq \int_0^{\infty} dx \\ &\times \frac{k_{0z} \exp[k_{0z}^2\sigma_2^2(x)] \cos(qx)}{(\kappa_z^2 - 2k_{0z}q)^{1/2}} \\ &\times \exp[-\sigma_2^2(x)(\kappa_z^2 - 2k_{0z}q)] \\ &\times \text{Erfc}[-i\sigma_2(x)(\kappa_z^2 - 2k_{0z}q)^{1/2}], \end{aligned} \quad (20a)$$

$$\begin{aligned} \Pi_{\text{refl}}^{\text{coh}} &= \frac{1}{4\pi} \int_{-\infty}^{\infty} dq \int_0^{\infty} dx \cos(qx) \\ &\times \left[\exp\left\{-\sigma_2^2(x)\left[(\kappa_z^2 - 2k_{0z}q)^{1/2} + k_{0z}\right]^2\right\} \right. \\ &\times \text{Erfc}\left\{-\frac{\varepsilon}{2\sigma_2(x)} - i\sigma_2(x)\left[(\kappa_z^2 - 2k_{0z}q)^{1/2} + k_{0z}\right]\right\} \\ &- \exp\left\{-\sigma_2^2(x)\left[(\kappa_z^2 - 2k_{0z}q)^{1/2} - k_{0z}\right]^2\right\} \\ &\times \text{Erfc}\left\{\frac{\varepsilon}{2\sigma_2(x)} - i\sigma_2(x)\left[(\kappa_z^2 - 2k_{0z}q)^{1/2} - k_{0z}\right]\right\} \\ &- \frac{k_{0z}}{(\kappa_z^2 - 2k_{0z}q)^{1/2}} \left(\exp\left\{-\sigma_2^2(x)\left[(\kappa_z^2 - 2k_{0z}q)^{1/2} + k_{0z}\right]^2\right\} \right. \\ &\times \text{Erfc}\left\{-i\sigma_2(x)\left[(\kappa_z^2 - 2k_{0z}q)^{1/2} + k_{0z}\right]\right\} \\ &+ \exp\left\{-\sigma_2^2(x)\left[(\kappa_z^2 - 2k_{0z}q)^{1/2} - k_{0z}\right]^2\right\} \\ &\left. \times \text{Erfc}\left\{-i\sigma_2(x)\left[(\kappa_z^2 - 2k_{0z}q)^{1/2} - k_{0z}\right]\right\} \right) \left. \right] \end{aligned} \quad (20b)$$

and

$$\begin{aligned} \Omega_{\text{tran}}^{\text{coh}} &= \frac{\exp[-\sigma^2(\kappa_z - k_{0z})^2/2]}{2\pi} \int_{-\infty}^{\infty} dq \int_0^{\infty} dx \\ &\times \frac{k_{0z} \exp[\sigma_2^2(x)(\kappa_z - k_{0z})^2/4] \cos(qx)}{(\kappa_z^2 - 2k_{0z}q)^{1/2}} \\ &\times \left(\exp\left\{-\sigma_2^2(x)\left[(\kappa_z^2 - 2k_{0z}q)^{1/2} - \frac{k_{0z} + \kappa_z}{2}\right]^2\right\} \right. \\ &\times \text{Erfc}\left\{-i\sigma_2(x)\left[(\kappa_z^2 - 2k_{0z}q)^{1/2} - \frac{k_{0z} + \kappa_z}{2}\right]\right\} \\ &+ \exp\left\{-\sigma_2^2(x)\left[(\kappa_z^2 - 2k_{0z}q)^{1/2} + \frac{k_{0z} + \kappa_z}{2}\right]^2\right\} \\ &\left. \times \text{Erfc}\left\{-i\sigma_2(x)\left[(\kappa_z^2 - 2k_{0z}q)^{1/2} + \frac{k_{0z} + \kappa_z}{2}\right]\right\} \right), \end{aligned} \quad (21a)$$

$$\begin{aligned} \Pi_{\text{tran}}^{\text{coh}} &= \frac{1}{4\pi} \int_{-\infty}^{\infty} dq \int_0^{\infty} dx \cos(qx) \\ &\times \left[\exp\left\{-\sigma_2^2(x)\left[(\kappa_z^2 - 2k_{0z}q)^{1/2} - \kappa_z\right]^2\right\} \right. \\ &\times \text{Erfc}\left\{-\frac{\varepsilon}{2\sigma_2(x)} - i\sigma_2(x)\left[(\kappa_z^2 - 2k_{0z}q)^{1/2} - \kappa_z\right]\right\} \\ &- \exp\left\{-\sigma_2^2(x)\left[(\kappa_z^2 - 2k_{0z}q)^{1/2} + \kappa_z\right]^2\right\} \\ &\times \text{Erfc}\left\{\frac{\varepsilon}{2\sigma_2(x)} - i\sigma_2(x)\left[(\kappa_z^2 - 2k_{0z}q)^{1/2} + \kappa_z\right]\right\} \\ &- \frac{k_{0z}}{(\kappa_z^2 - 2k_{0z}q)^{1/2}} \\ &\times \left(\exp\left\{-\sigma_2^2(x)\left[(\kappa_z^2 - 2k_{0z}q)^{1/2} - \kappa_z\right]^2\right\} \right. \\ &\times \text{Erfc}\left\{-i\sigma_2(x)\left[(\kappa_z^2 - 2k_{0z}q)^{1/2} - \kappa_z\right]\right\} \\ &+ \exp\left\{-\sigma_2^2(x)\left[(\kappa_z^2 - 2k_{0z}q)^{1/2} + \kappa_z\right]^2\right\} \\ &\left. \times \text{Erfc}\left\{-i\sigma_2(x)\left[(\kappa_z^2 - 2k_{0z}q)^{1/2} + \kappa_z\right]\right\} \right) \left. \right]. \end{aligned} \quad (21b)$$

The general formulae (20) and (21) obtained for the coefficients $\Omega_{\text{refl}}^{\text{coh}}$, $\Pi_{\text{refl}}^{\text{coh}}$, $\Omega_{\text{tran}}^{\text{coh}}$ and $\Pi_{\text{tran}}^{\text{coh}}$ complete the mathematical foundation for evaluating the reflection R^{coh} and transmission T^{coh} coefficients of the specular wave [cf. equations (14) and (15)].

Loosely speaking, the key ideas of the present theoretical approach are based on two major physical prerequisites. One of them is that implementing Kirchhoff's integral equation [cf. (1)] along with the Green function formalism [cf. (6), (7)] for describing the grazing X-ray scattering from a rough surface is very important. Another is that applying the rough-surface model (8) seems to be very effective for providing the statistical average of the rigorous solutions for the reflected and transmitted wave amplitudes in the form of expansion series (6)–(7).

As follows from formulae (14)–(15) and (20)–(21), in the limiting case of correlation length $\xi \rightarrow \infty$ they provide the reflection R^{coh} and transmission T^{coh} coefficients in the form of the conventional Fresnel coefficients R^{Fres} and T^{Fres} multiplied by the Debye–Waller factors $f_R = \exp(-2\sigma^2 k_{0z}^2)$ and $f_T = \exp[-\sigma^2(k_{0z} - \kappa_z)^2/2]$, respectively.

For the opposite case, in the extreme case when the correlation length $\xi = 0$, formulae (20) and (21) yield solutions for the reflection and transmission coefficients in the analytical form

$$R_{\xi=0}^{\text{coh}} = -\exp(-2\sigma^2 k_{0z}^2) + \frac{\Omega_{\text{refl},\xi=0}^{\text{coh}}}{1 - \Pi_{\text{refl},\xi=0}^{\text{coh}}}, \quad (22)$$

where the coefficients $\Omega_{\text{refl},\xi=0}^{\text{coh}}$ and $\Pi_{\text{refl},\xi=0}^{\text{coh}}$ are equal to

$$\Omega_{\text{refl},\xi=0}^{\text{coh}} = \exp(-\sigma^2 \kappa_z^2) (k_{0z}/\kappa_z) \text{Erfc}(-i\kappa_z \sigma),$$

$$\begin{aligned} \Pi_{\text{refl}, \xi=0}^{\text{coh}} = & \frac{1}{4} \left\{ \exp\left[-\sigma^2(\kappa_z + k_{0z})^2\right] \text{Erfc}\left[-\frac{\varepsilon}{2\sigma} - i\sigma(\kappa_z + k_{0z})\right] \right. \\ & - \exp\left[-\sigma^2(\kappa_z - k_{0z})^2\right] \text{Erfc}\left[\frac{\varepsilon}{2\sigma} - i\sigma(\kappa_z - k_{0z})\right] \\ & - \frac{k_{0z}}{\kappa_z} \left(\exp\left[-\sigma^2(\kappa_z + k_{0z})^2\right] \right. \\ & \times \text{Erfc}\left[-i\sigma(\kappa_z + k_{0z})\right] + \exp\left[-\sigma^2(\kappa_z - k_{0z})^2\right] \\ & \left. \left. \times \text{Erfc}\left[-i\sigma(\kappa_z - k_{0z})\right] \right) \right\} \end{aligned}$$

and

$$T_{\xi=0}^{\text{coh}} = \frac{\Omega_{\text{tran}, \xi=0}^{\text{coh}}}{1 - \Pi_{\text{tran}, \xi=0}^{\text{coh}}}, \quad (23)$$

where the coefficients $\Omega_{\text{tran}, \xi=0}^{\text{coh}}$, $\Pi_{\text{tran}, \xi=0}^{\text{coh}}$ are equal to

$$\begin{aligned} \Omega_{\text{tran}, \xi=0}^{\text{coh}} = & \frac{1}{2} \exp\left[-\frac{\sigma^2(\kappa_z - k_{0z})^2}{4}\right] \\ & \times \frac{k_{0z}}{\kappa_z} \left\{ \exp\left[-\frac{\sigma^2(\kappa_z - k_{0z})^2}{4}\right] \right. \\ & \times \text{Erfc}\left[-i\frac{\sigma(\kappa_z - k_{0z})}{2}\right] \\ & + \exp\left[-\frac{\sigma^2(3\kappa_z + k_{0z})^2}{4}\right] \\ & \left. \times \text{Erfc}\left[-i\frac{\sigma(3\kappa_z + k_{0z})}{2}\right] \right\}, \end{aligned}$$

$$\begin{aligned} \Pi_{\text{tran}, \xi=0}^{\text{coh}} = & \frac{1}{4} \left\{ \text{Erfc}\left(\frac{-\varepsilon}{2\sigma}\right) - \exp(-4\sigma^2\kappa_z^2) \text{Erfc}\left(\frac{\varepsilon}{2\sigma} - i2\sigma\kappa_z\right) \right. \\ & \left. - \frac{k_{0z}}{\kappa_z} [1 + \exp(-4\sigma^2\kappa_z^2) \text{Erfc}(-2i\sigma\kappa_z)] \right\}, \end{aligned}$$

respectively.

In the case of finite correlation lengths ξ the numerical run-through for calculating the reflection $|R^{\text{coh}}(\theta)|^2$ and transmission $|T^{\text{coh}}(\theta)|^2$ scans versus the X-ray incidence angle θ is carried out and based on the theoretical formulae (14), (15), (20)–(21).

Before proceeding further, a simple analysis shows that the integrands in integrals (20) and (21) essentially depend on the ‘combined’ r.m.s. roughness $\sigma_2(x)$. It does mean that, up to a certain extent, increasing (decreasing) the r.m.s. roughness σ is equivalent to decreasing (increasing) the correlation length ξ .

In the general case the following parameters are used for the numerical run-through of the reflection and transmission scans as functions of the X-ray incidence angle θ . Namely, (i) the complex electric susceptibility of a medium χ equal to $-10^{-5}(1 - 0, 05i)$, (ii) the r.m.s. roughness σ measured in units of $\lambda/2\pi$, (iii) the correlation length ξ measured in units of the X-ray absorption length $l = \lambda/[2\pi \text{Im}(\chi)] = 2 \times 10^6 \lambda/2\pi$ in a medium, (iv) the X-ray incidence angle θ plotted in units of 0.009° , and a $\{\theta\}$ array size equal to 60.

Based on the theoretical formulae (14), (15) and (20)–(21) the scans of $-\ln[|R^{\text{coh}}(\theta)|^2]$ and $|T^{\text{coh}}(\theta)|^2$ were numerically

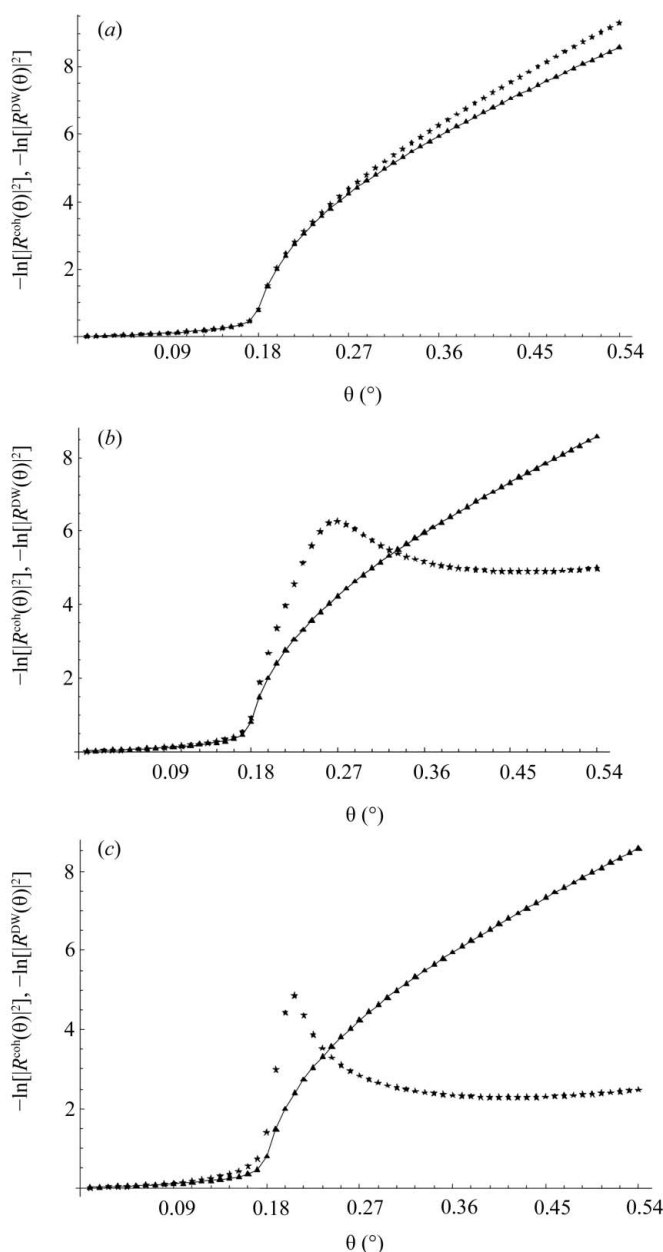
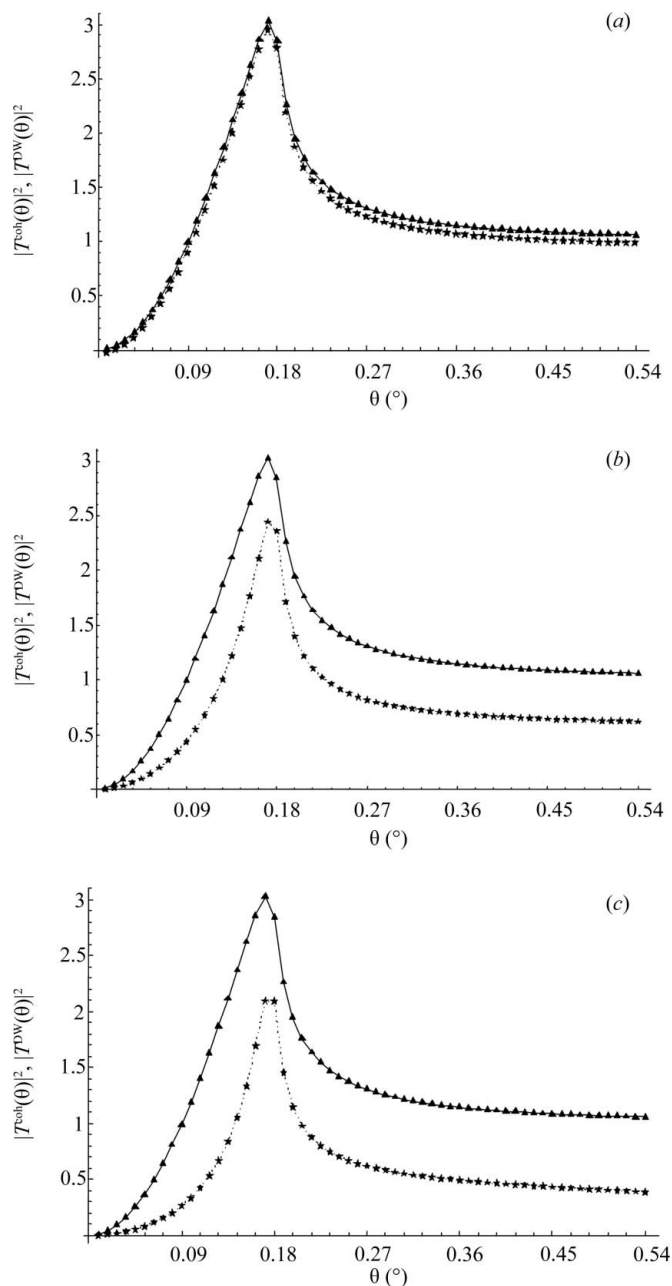


Figure 2

The numerically calculated reflectance $-\ln[|R^{\text{coh}}(\theta)|^2]$ scans (stars). The dimensionless correlation length ξ/l is equal to (a) 100, (b) 1, (c) 0, where l is the X-ray absorption length in the medium, $l = \lambda/[2\pi \text{Im}(\chi)]$. The r.m.s. roughness σ is equal to $65(\lambda/2\pi)$. The reflectance $-\ln|R^{\text{Dw}}(\theta)|^2$ scans related to the Debye–Waller approximation are drawn with full lines (with points) as well.

calculated for the different parameter values: the correlation length $\{\xi\}$ array = $l\{0, 1, 100\}$ and the r.m.s. roughness $\{\sigma\}$ array = $\lambda/2\pi \{25, 65, 85\}$.

As an example, the numerical run-through reflection and transmission scan data are depicted in Figs. 2(a), 2(b) and 2(c) for $-\ln[|R^{\text{coh}}(\theta)|^2]$ and in Figs. 3(a), 3(b) and 3(c) for $|T^{\text{coh}}(\theta)|^2$. The r.m.s. roughness σ is chosen to be equal to $65(\lambda/2\pi)$ and the correlation length ξ divided by l is sequentially equal to (a) = 100, (b) = 1 and (c) = 0.


Figure 3

The numerically calculated transmission $|T^{\text{coh}}(\theta)|^2$ scans (stars). The dimensionless correlation length ξ/l is equal to (a) 100, (b) 1, (c) 0, where l is the X-ray absorption length in the medium, $l = \lambda/[2\pi \text{Im}(\chi)]$. The r.m.s. roughness σ is equal to $65(\lambda/2\pi)$. The transmission $|T^{\text{DW}}(\theta)|^2$ scans related to the Debye–Waller approximation are drawn with full lines (with points) as well.

Note that the logarithmic scale of the reflection angular scans, $-\ln[|R^{\text{coh}}(\theta)|^2]$, along the ordinates is chosen in order to reveal their behavior outside the total reflection angular region, $\theta > \theta_{\text{Cr}}$.

To be specific, the numerical run-through of the $-\ln[|R^{\text{coh}}(\theta)|^2]$ and $|T^{\text{coh}}(\theta)|^2$ scans depicted in Figs. 2 and 3 clearly show that multiple diffuse X-ray scattering effects notably influence the reflection and transmission coefficients of the specular wave at large incidence angles, $\theta > \theta_{\text{Cr}}$, outside

the total X-ray reflection region, and they drastically become stronger with reducing correlation length $\xi \leq l$ [see Figs. 2(b) and 2(c) and Figs. 3(b) and 3(c)].

5. Concluding remarks

The goal of our study was to consider the grazing X-ray specular scattering from rough surfaces based on the Green function formalism. For this, Kirchhoff's integral equation (1) allows us to describe the wavefield propagation within a single surface-confined medium and it is adjusted with the Gaussian statistical model of a rough surface using the two-point height–height roughness correlation function.

The reflection $R^{\text{coh}}(\theta)$ and transmission $T^{\text{coh}}(\theta)$ coefficients of the specular wave have been obtained by the present theoretical approach. This allows us to take into account the multiple diffuse X-ray scattering effects and then to reveal their influence upon grazing X-ray specular scattering from statistically rough surfaces. Presumably an ensemble of random surface heights described in the frame of Gaussian statistics may be a good model of a real solid rough surface (*cf.* Sinha *et al.*, 1988).

The reflection $|R^{\text{coh}}(\theta)|^2$ and transmission $|T^{\text{coh}}(\theta)|^2$ scans are numerically calculated for finite correlation lengths ξ . It is shown that multiple diffuse X-ray scattering effects lead to the re-emergence of the X-ray specular wave, at least at large incidence angles, $\theta > \theta_{\text{Cr}}$, outside the total reflection region.

The influence of multiple diffuse scattering effects upon the grazing X-ray specular scattering is essential for the correlation lengths ξ that are of the order of, and/or less than, the X-ray absorption length in a medium l .

On the other hand, it should be mentioned that the general formulae (14)–(15) and (20)–(21) for calculating the reflection $|R^{\text{coh}}(\theta)|^2$ and transmission $|T^{\text{coh}}(\theta)|^2$ scans might be useful for obtaining information about the two-point height–height correlation functions of real rough surfaces.

Of greater interest may be future studies in terms of justifying the present theoretical approach for deriving the reflection and transmission coefficients of the specular wave by use of the statistical cumulant average technique (see, for example, Poliakov *et al.*, 1991). At the same time, implementing high-resolution diffuse scattering (Lazzari, 2002) offers a new possibility to probe surfaces and/or interfaces produced by various growth processes and then examining their roughness characteristics on a length scale of the order of the correlation length ξ .

The authors would like to thank V. L. Nosik and S. V. Salikhov for useful discussions and comments.

References

- Boer, D. K. G. de (1994). *Phys. Rev. B*, **49**, 5817–5823.
- Boer, D. K. G. de (1995). *Phys. Rev.* **51**, 5297–5305.
- Bridou, F., Gautier, J., Delmotte, F., Ravet, M.-F., Durand, O. & Modreanu, M. (2006). *Appl. Surf. Sci.* **253**, 12–16.

- Bushuev, V. A., Lomov, A. A. & Sutyurin, A. G. (2002). *Crystallogr. Rep.* **47**, 683–690.
- Chukhovskii, F. N. (2009). *Acta Cryst.* **A65**, 39–45.
- Hodroj, A., Roussel, H., Crisci, A., Robaut, F., Gottlieb, U. & Deschanvres, J. L. (2006). *Appl. Surf. Sci.* **253**, 363–366.
- Holy, V., Pietsch, U. & Baumbach, T. (1999). *High-Resolution X-ray Scattering from Thin Films and Multilayers*. Berlin: Springer Verlag.
- Kohn, V. G. (2003). *Poverkhnost*, **1**, 23–27.
- Lazzari, R. (2002). *J. Appl. Cryst.* **35**, 406–421.
- Lomov, A. A., Sutyurin, A. G., Prokhorov, D. Yu., Galiev, G. B., Khabarov, Yu. V., Chuev, M. A. & Imamov, R. M. (2005). *Crystallogr. Rep.* **50**, 739–750.
- Nevot, L. & Croce, P. (1980). *Rev. Phys. Appl.* **15**, 761–779.
- Nosik, V. L. (2002). *Crystallogr. Rep.* **47**, 925–933.
- Petrashen', P. V., Kov'ev, E. K., Chukhovskii, F. N. & Degtyarev, Yu. L. (1983). *Solid State Phys.* **25**, 1211–1214.
- Poliakov, A. M., Chukhovskii, F. N. & Piskunov, D. I. (1991). *Sov. Phys. JETP*, **72**, 330–340.
- Schmidbauer, M., Schäfer, P., Besedin, S., Grigoriev, D., Köhler, R. & Hanke, M. (2008). *J. Synchrotron Rad.* **15**, 549–557.
- Sinha, S. K., Sirota, E. B., Garoff, S. & Stanley, H. B. (1988). *Phys. Rev. B*, **38**, 2297–2311.
- Sutyurin, A. G. & Prokhorov, D. Yu. (2006). *Crystallogr. Rep.* **51**, 570–576.
- Yoneda, Y. (1963). *Phys. Rev.* **131**, 2010–2013.
- Zozulya, A. V., Yefanov, O. M., Vartanyants, I. A., Mundboth, K., Mocuta, C., Metzger, T. H., Stangl, J., Bauer, G., Boeck, T. & Schmidbauer, M. (2008). *Phys. Rev. B*, **78**, 121304.